ELSEVIER

Physica B 215 (1995) 329–336

PHYSICA B

Neutron reflection interferometry: Extraction of the phase in total reflection from stratified media

John Lekner

Department of Physics, Victoria University of Wellington, Wellington, New Zealand

Received 9 March 1995

Abstract

Lloyd's mirror configuration has been suggested for determination of the reflection phase, in order to obtain information about the reflecting stratification. For thermal neutrons total reflection occurs at small glancing angles. We show that the phase of the reflection amplitude in total reflection is linear in the glancing angle at small angles, and determine the coefficient of proportionality for three solvable variations of the scattering length density. The semiclassical reflection phase is shown to fail at grazing incidence, but, for smooth profiles which are thick compared to the neutron wavelength, may have a useful range of glancing angles smaller than the critical angle.

1. Introduction

Lloyd's mirror experiment [1] produces interference fringes between a direct and a reflected beam, providing information about their relative phase. Klein, Opat and collaborators have suggested Lloyd's mirror configuration for neutrons [2], and implemented it for light [3]. They used the semiclassical short-wave limit for the reflection phase

$$\delta \approx \delta_a = 2\int_0^{z_0} dz\, q(z) - \pi/2, \tag{1}$$

where $q(z)$ is the local value of the normal component of the wave vector, and z_0 is the classical turning point at which q is zero (see for example Ref. [4, Sections 6–7 and A-6, Eq. (113)]). This approximation is known to fail at grazing incidence, where the effective wavelength $2\pi/q$ is large; see Figs. 6–9 and the accompanying discussion in Ref. [4]. Since the Lloyd mirror experiment for neutrons must be performed at glancing angles θ smaller than the critical angle θ_c for total reflection, and θ_c is typically of the order of one degree for neutrons of 10 Å wave-length [5], we need to examine the behaviour of the reflection phase δ at small glancing angles. We shall show that, in all cases,

$$\delta = \pm\pi + c\theta + O(\theta^3), \tag{2}$$

where the coefficient c is determined mainly by the variation in scattering length density at the outer boundary of the reflecting stratification. The initial variation in the reflecting medium is important at glancing incidence, because the neutron wave penetrates only to a distance of order z_0, which goes to zero at grazing incidence.

At grazing incidence ($\theta \to 0$) Eq. (2) correctly gives the reflection amplitude $r = e^{i\delta} \to -1$, in agreement with the general result of Ref. [4, Section 2–3], whereas Eq. (1) gives $r \to -i$. As we shall see, the short-wave formula (1) also fails to give the correct θ-dependence at small θ.

SSDI 0921-4526(95)00425-4

2. A general formula for the total reflection phase

Let neutrons of wavelength λ be incident from vacuum onto a stratified layer situated between $z = 0$ and $z = \Delta z$. The scattering length density $\rho = b/v$ (b is the bound scattering length, and v is the volume per scatterer) is assumed to be a function of z only. Then the wave equation for the neutrons separates: if the neutrons travel in the zx plane, the wave function is (approximately) the modulated plane wave $\exp(\mathrm{i}Kx)\psi(z)$, where ψ satisfies

$$\frac{\mathrm{d}^2\psi}{\mathrm{d}z^2} + q^2(z)\psi = 0, \qquad q^2(z) = q_1^2 - 4\pi\rho(z), \tag{3}$$

with

$$q_1 = \frac{2\pi}{\lambda}\sin\theta, \qquad K = \frac{2\pi}{\lambda}\cos\theta, \tag{4}$$

being the normal and tangential components of the wave vector in the medium of incidence. Because of the translational invariance in the x-direction, K is a constant of the motion, while $q(z)$ is not. The classical turning point z_0 is given by $q(z_0) = 0$, which implies

$$q_1^2 = 4\pi\rho(z_0) \quad \text{or} \quad \rho(z_0) = \pi\sin^2\theta/\lambda^2. \tag{5}$$

The z-dependence of the wave function can be written as

$$\psi(z) = \begin{cases} \mathrm{e}^{\mathrm{i}q_1 z} + r\mathrm{e}^{\mathrm{i}q_1 z}, & z \leqslant 0, \\ \alpha F(z) + \beta G(z), & 0 < z < \Delta z, \\ t\mathrm{e}^{\mathrm{i}q_2 z}, & z \geqslant \Delta z, \end{cases} \tag{6}$$

where r and t are the reflection and transmission amplitudes, and $F(z)$ and $G(z)$ are linearly independent solutions of Eq. (3) within the reflecting layer. The substrate is assumed to be homogeneous, with scattering length density ρ_2, so that

$$q_2^2 = q_1^2 - 4\pi\rho_2 \equiv q_1^2 - q_c^2. \tag{7}$$

The critical angle θ_c is defined by $q_2 = 0$, so that

$$\sin^2\theta_c = \lambda^2\rho_2/\pi. \tag{8}$$

For $\theta < \theta_c$ the neutrons are totally reflected, with exponential decay (evanescence) into the substrate according to $\exp(-|q_2|z)$, where

$$|q_2| = (4\pi\rho_2 - q_1^2)^{1/2} = \frac{2\pi}{\lambda}(\sin^2\theta_c - \sin^2\theta)^{1/2}. \tag{9}$$

The continuity of ψ and $\mathrm{d}\psi/\mathrm{d}z$ at $z = 0$ and $z = \Delta z$ gives four equations, which can be solved for the four unknowns r, t, α and β in Eq. (6). We find (cf. Eq. (2.25) of Ref. [4]):

$$r = \frac{q_1 q_2(F,G) + \mathrm{i}q_1(F,G') + \mathrm{i}q_2(F',G) - (F',G')}{q_1 q_2(F,G) + \mathrm{i}q_1(F,G') - \mathrm{i}q_2(F',G) + (F',G')}, \tag{10}$$

where

$$\begin{aligned} (F,G) &\equiv F_1G_2 - G_1F_2, \\ (F,G') &\equiv F_1G_2' - G_1F_2', \\ (F',G) &\equiv F_1'G_2 - G_1'F_2, \\ (F',G') &\equiv F_1'G_2' - G_1'F_2', \end{aligned} \tag{11}$$

and $F_1 = F(0+)$, $F_2 = F(\Delta z-)$, $F_1' = \mathrm{d}F/\mathrm{d}z$ evaluated at $z = 0+$, etc. We see that $r \to -1$ as $q_1 \to 0$, as stated above. When $\theta < \theta_c$, $q_2 = \mathrm{i}|q_2|$ and

$$r = \frac{q_1[(F,G') + |q_2|(F,G)] + \mathrm{i}[(F',G') + |q_2|(F',G)]}{q_1[(F,G') + |q_2|(F,G)] - \mathrm{i}[(F',G') + |q_2|(F',G)]}. \tag{12}$$

The wave equation (3) is linear, with real coefficients. Thus the functions $F(z)$ and $G(z)$ may be chosen to be real, in which case the phase of r ($r = \mathrm{e}^{\mathrm{i}\delta}$ for $\theta < \theta_c$) is given by

$$\delta = 2\arctan\left\{\frac{(F',G') + |q_2|(F',G)}{q_1[(F,G') + |q_2|(F,G)]}\right\} \equiv 2\arctan\left(\frac{Q}{q_1}\right). \tag{13}$$

Since

$$\arctan(X) = \mathrm{sgn}(X)\pi/2 - X^{-1} + \mathrm{O}(X^{-3}), \tag{14}$$

we see that

$$\delta = \pi\,\mathrm{sgn}(Q_0) - \frac{2q_1}{Q_0} + \mathrm{O}\left(\frac{q_1}{Q_0}\right)^3 \tag{15}$$

with Q_0 equal to the limiting value of Q as $q_1 \to 0$ at grazing incidence, where, from Eq. (9),

$$|q_2| \to q_c = (4\pi\rho_2)^{1/2} = \frac{2\pi}{\lambda}\sin\theta_c \tag{16}$$

(for $q_1 < q_c$ we have $|q_2| = (q_c^2 - q_1^2)^{1/2}$). Since $q_1 = (2\pi/\lambda)\sin\theta$, Eq. (15) proves Eq. (2) for reflecting profiles of finite thickness.

We now look at some examples of the behaviour of the phase δ.

3. Exact total reflection phase for three profiles

We will give explicit formulae for the phase δ in total reflection, i.e. for $q_1 < q_c = (4\pi\rho_2)^{1/2}$, for the three variations of the scattering density $\rho(z)$ shown in Fig. 1.

3.1. Homogeneous layer

When $\theta < \theta_a$ where $\sin^2\theta_a = \lambda^2\rho_a/\pi$, $q = (2\pi\mathrm{i}/\lambda) \times (\sin^2\theta_a - \sin^2\theta)^{1/2} = \mathrm{i}|q|$ and the solutions of the wave equation within the layer are $F(z) = \mathrm{e}^{-|q|z}$ and $G(z) = \mathrm{e}^{+|q|z}$. Then, with

$$C \equiv \cosh|q|\Delta z, \qquad S = \sinh|q|\Delta z, \tag{17}$$

we have

$$\begin{aligned}(F,G) &= 2S, & (F',G') &= -2|q|^2 S,\\ (F,G') &= 2|q|C, & (F',G) &= -2|q|C.\end{aligned} \tag{18}$$

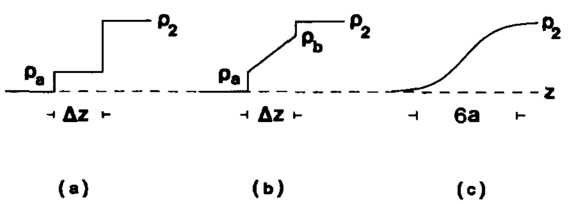

Fig. 1. Three scattering density profiles for which the total reflection phase is calculated: (a) homogeneous layer; (b) linear variation of $\rho(z)$; (c) $\rho = \rho_2/(1 + \mathrm{e}^{-z/a})$.

Thus the function Q defined in Eq. (13) is

$$Q = -|q|\left(\frac{T + |q_2|/|q|}{1 + T|q_2|/|q|}\right), \tag{19}$$

where $T = \tanh(|q|\Delta z)$. As $q_1 \to 0$, $|q_2| \to q_c$ and $|q| \to q_a = (2\pi/\lambda)\sin\theta_a$, so

$$Q \to Q_0 = -q_a\frac{\tanh(q_a\Delta z) + q_c/q_a}{1 + (q_c/q_a)\tanh(q_a\Delta z)}. \tag{20}$$

This varies between $-q_c$ (when $q_a\Delta z \ll 1$) and $-q_a$ (when $q_a\Delta z \gg 1$).

If $\rho_a < \rho_2$ and $\theta_a < \theta < \theta_c$, $q = (2\pi/\lambda)(\sin^2\theta - \sin^2\theta_a)^{1/2}$ is real and the appropriate solutions are $F(z) = \cos qz$ and $G(z) = \sin qz$. Then with

$$c = \cos q\Delta z, \qquad s = \sin q\Delta z, \tag{21}$$

we find

$$\begin{aligned}(F,G) &= s, & (F',G') &= q^2 s,\\ (F,G') &= qc, & (F',G) &= -qc.\end{aligned} \tag{22}$$

The function Q which gives $\delta = 2\arctan(Q/q_1)$ is now

$$Q = q\tan[q\Delta z - \arctan(|q_2|/q)]. \tag{23}$$

At $\theta = \theta_a$ the normal component of the wave vector within the layer is zero, and both Eqs. (19) and (23) give

$$Q(\theta = \theta_a) = \frac{-1}{\Delta z + 1/|q_2(\theta_a)|}. \tag{24}$$

From Eq. (20) we conclude that Q_0 is negative, so at grazing angles of incidence the reflection phase increases linearly with θ from $-\pi$. When $\rho_a = \rho_2$ the layer does not reflect (it is identical to the substrate as far as the neutrons are concerned). Then $|q| = |q_2|$ and we regain the bare substrate phase

$$\delta = -2\arctan(|q_2|/q_1) \tag{25}$$

in accord with the reflection amplitude $(q_1 - \mathrm{i}|q_2|)/(q_1 + \mathrm{i}|q_2|)$.

From Eqs. (24) and (13) we see that

$$\delta(\theta_a) = 2\arctan\left[\frac{-1}{q_a\Delta z + q_a/(q_c^2 - q_a^2)^{1/2}}\right]. \tag{26}$$

Thus $\delta(\theta)$ changes by at most π as θ increases from zero to θ_a. It follows that if many Lloyd fringes are to be seen, they have to be in the region $\theta_a < \theta < \theta_c$, where the neutron wave function is oscillatory within the layer (we assume that $\rho_a < \rho_2$). The parameter which determines the number of fringes is, from Eq. (23),

$$(q_c^2 - q_a^2)^{1/2}\Delta z = [4\pi(\rho_2 - \rho_a)]^{1/2}\Delta z, \tag{27}$$

since q increases from zero to $(q_c^2 - q_a^2)^{1/2}$ as θ increases from θ_a to θ_c. An additional fringe appears for each increment of this parameter through an odd multiple of $\pi/2$; thus a count of the fringes gives an estimate of the quantity (27) (see Section 4 for a discussion of other contributions to the total phase). Fig. 2 shows the total reflection phase δ for a layer of silicon on iron.

3.2. Linear profile

We now consider the scattering length density profile shown in Fig. 1(b). When $\rho(z)$ is linear in z, so is $q^2(z) = q_1^2 - 4\pi\rho(z)$. We change to

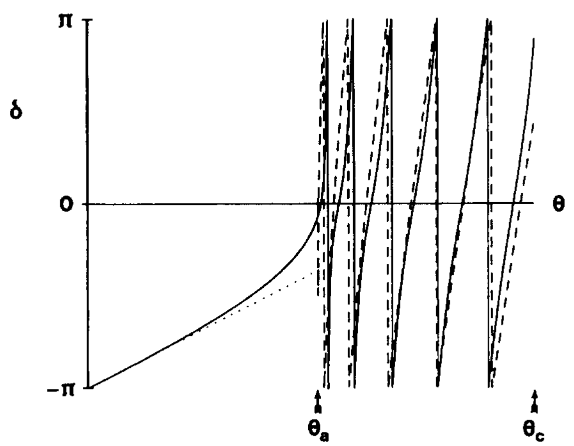

Fig. 2. The phase of the reflection amplitude for a 318λ layer of silicon ($\rho_a = 0.215 \times 10^{-5}$ Å^{-2}) on iron ($\rho_2 = 0.805 \times 10^{-5}$ Å^{-2}). For neutrons of 6.28 Å wavelength, $\Delta z \approx 2000$ Å, $\theta_a \approx 0.3°$ and $\theta_c \approx 0.5°$. The dotted line is calculated from Eqs. (15) and (20). The dashed curve shows the semiclassical phase $2\int_0^{z_0} dz\, q(z) - \pi/2 = 2(q_1^2 - q_a^2)^{1/2}\Delta z - \pi/2$ (for $\theta_a \leqslant \theta \leqslant \theta_c$).

[6] the variable

$$\zeta(z) = \left(\frac{1}{4\pi}\left|\frac{\Delta z}{\Delta\rho}\right|\right)^{2/3} q^2(z) = \left|\frac{\Delta z}{\Delta q^2}\right|^{2/3} q^2(z) \equiv q^2(z)/k^2, \tag{28}$$

where $\Delta\rho = \rho_b - \rho_a$. The wave equation (3) transforms to

$$\frac{d^2\psi}{d\zeta^2} + \zeta\psi = 0 \tag{29}$$

with solutions $\mathrm{Ai}(-\zeta)$ and $\mathrm{Bi}(-\zeta)$, the Airy functions [7]. These functions, and their derivatives, need to be evaluated at the end points

$$\zeta_a = (q_1^2 - 4\pi\rho_a)/k^2, \qquad \zeta_b = (q_1^2 - 4\pi\rho_b)/k^2. \tag{30}$$

For definiteness we will assume $0 < \rho_a < \rho_b < \rho_2$ in the discussion that follows. At grazing incidence both ζ_a and ζ_b are negative, and the functions $F(z) = \mathrm{Ai}(-\zeta)$ and $G(z) = \mathrm{Bi}(-\zeta)$ respectively decrease and increase monotonically from $z = 0$ to Δz. At θ_a defined by $\sin^2\theta_a = \lambda^2\rho_a/\pi$ the end point ζ_a is zero. For $\theta_a < \theta < \theta_b = \arcsin(\lambda^2\rho_b/\pi)^{1/2}$ the functions F and G change from oscillatory to monotonic behaviour at the classical turning point z_0 defined in Eq. (5). The turning point moves from $z = 0$ to $z = \Delta z$ as θ increases from θ_a to θ_b. Before the turning point the Airy functions are, for large argument, proportional to $\zeta^{-1/2}$ times the sine or cosine of $\frac{2}{3}\zeta^{3/2} + \pi/4$. From Eq. (20), $\frac{2}{3}\zeta^{3/2} = (\Delta z/\Delta\rho)q^3/6\pi$; thus the dimensionless parameter

$$\frac{1}{6\pi}\frac{\Delta z}{\Delta\rho}(q_b^2 - q_a^2)^{3/2} = \frac{4\sqrt{\pi}}{3}(\rho_b - \rho_a)^{1/2}\Delta z \tag{31}$$

determines the number of Lloyd fringes seen for $\theta \leqslant \theta_b$ (an additional fringe appears for each increment of this parameter by 2π). We note that, as in the case of the corresponding fringe counting parameter (27) for a homogeneous layer, the fringe number is independent of the neutron wavelength: for shorter wavelengths the same number of fringes is compressed into a narrower angular range.

The short-wave approximation to the phase, $\delta_a = 2\int_0^{z_0} dz\, q(z) - \pi/2$ can be evaluated analytically.

We find

$$\int_0^{z_0} \mathrm{d}z\, q(z) = \tag{32}$$

$$\begin{cases} 0, & \theta \leqslant \theta_a, \\ \dfrac{1}{6\pi}\dfrac{\Delta z}{\Delta\rho}(q_1^2 - q_a^2)^{3/2}, & \theta_a \leqslant \theta \leqslant \theta_b, \\ \dfrac{1}{6\pi}\dfrac{\Delta z}{\Delta\rho}\{(q_1^2 - q_a^2)^{3/2} - (q_1^2 - q_b^2)^{3/2}\}, & \theta_b \leqslant \theta \leqslant \theta_c, \end{cases}$$

As $\Delta\rho = \rho_b - \rho_a$ tends to zero, this reduces to the homogeneous layer phase integral

$$\int_0^{z_0} \mathrm{d}z\, q(z) = \begin{cases} 0, & \theta \leqslant \theta_a, \\ (q_1^2 - q_a^2)^{1/2}\Delta z, & \theta_a \leqslant \theta \leqslant \theta_c. \end{cases} \tag{33}$$

The exact phase and the short-wave approximate phase are compared in Fig. 3. In calculating the exact phase from Eq. (13) we need derivatives of the Airy functions with respect to z. These are related to the ζ derivatives via

$$\begin{aligned} \frac{\mathrm{d}}{\mathrm{d}z} &= -\,\mathrm{sgn}\left(\frac{\Delta\rho}{\Delta z}\right)k\frac{\mathrm{d}}{\mathrm{d}\zeta} \\ &= -\,\mathrm{sgn}\left(\frac{\Delta\rho}{\Delta z}\right)\left(4\pi\left|\frac{\Delta\rho}{\Delta z}\right|\right)^{1/3}\frac{\mathrm{d}}{\mathrm{d}\zeta}. \end{aligned} \tag{34}$$

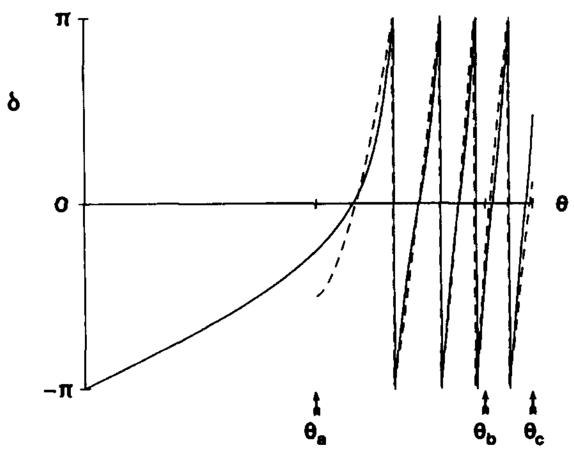

Fig. 3. Comparison of the exact and semiclassical reflection phases for the linear ramp profile of Fig. 1(b), with $\rho_a = 0.215$, $\rho_b = 0.644$ and $\rho_2 = 0.805$ (units of 10^{-5} Å^{-2}) for a layer thickness $\Delta z = 318\lambda$ (this corresponds to 2000 Å for $\lambda = 2\pi$Å). The full curve is the exact phase, the dashed curve the short-wave approximation.

3.3. Hyperbolic tangent profile

In contrast to the two profiles just considered, the profile

$$\rho(z) = \frac{\rho}{1 + \mathrm{e}^{-z/a}} = \tfrac{1}{2}\rho_2[1 + \tanh(z/2a)] \tag{35}$$

has no finite boundaries. Since $\mathrm{e}^3 \approx 20$, $\rho(z)$ varies from about 5% to about 95% of ρ_2 as z increases from $-3a$ to $+3a$. From Ref. [8] or directly from the formula (10.44) of Ref. [4] we find for this profile the total reflection phase

$$\begin{aligned} \delta = 2\sum_{n=1}^{\infty} \arctan\left\{\frac{2y_1 y_c^2}{n(n^2 + 4y_1^2 - y_c^2)}\right\} \\ - 2\arctan\left(\frac{\tan\pi|y_2|}{\tanh\pi y_1}\right), \end{aligned} \tag{36}$$

where

$$\begin{aligned} y_1 &= q_1 a, \\ |y_2| &= |q_2|a = (q_c^2 - q_1^2)^{1/2}a \equiv (y_c^2 - y_1^2)^{1/2}. \end{aligned} \tag{37}$$

The leading terms at grazing incidence are (from Eqs. (14) and (36), setting $|y_2| \to q_c a \equiv y_c$):

$$\begin{aligned} \delta = &-\pi\,\mathrm{sgn}(\tan\pi y_c) \\ &+ 2y_1\left\{\frac{\pi}{\tan\pi y_c} + \sum_{n=1}^{\infty}\frac{2y_c^2}{n(n^2 - y_c^2)}\right\} + \mathrm{O}(y_1^3). \end{aligned} \tag{38}$$

The infinite sum in Eq. (38) may be expressed in terms of the psi function $\Psi = \Gamma'/\Gamma$, since (Ref. [7, Eq. (6.3.16)])

$$\Psi(1 + z) = -\gamma + \sum_{n=1}^{\infty}\frac{n}{n(n + z)} \quad (z \neq \text{negative integer}), \tag{39}$$

where $\gamma = 0.5772\ldots$ is Euler's constant. Thus

$$\sum_{n=1}^{\infty}\frac{2y_c^2}{n(n^2 - y_c^2)} = -\{2\gamma + \Psi(1 + y_c) + \Psi(1 - y_c)\}. \tag{40}$$

The apparent singularity at integer y_c is removable: on using the reflection formula (Ref. [7, Eq. (6.3.7)])

$$\Psi(1 - z) = \Psi(z) + \pi\cot\pi z, \tag{41}$$

Eq. (38) reduces to

$$\delta = -\pi\,\mathrm{sgn}(\tan \pi y_c) - 2y_1\{2\gamma + \Psi(y_c) + \Psi(1 + y_c)\} + O(y_1^3). \qquad (42)$$

This formula demonstrates that the grazing incidence form (2) of the total reflection phase is not restricted to profiles of finite extent.

The semiclassical phase formula (1) applies to profiles which have $q(z) = q_1$ for $z \leqslant 0$ (see Section A-6 of Ref. [4]). This is not the case for the profile (35); the appropriate short-wave phase has been evaluated in Ref. [4, Eq. (6.129)]. It is

$$\delta_a = 4y_1 \log\left(\frac{2y_1}{y_c}\right) - \pi/2 - 4|y_2| \arctan\left(\frac{y_1}{|y_2|}\right). \qquad (43)$$

At the critical angle, the Euler–Maclaurin summation formula (Ref. [7], Eq. (3.6.28)) gives $\delta(\theta_c) = 4y_c \log 2 - \pi/2 + (4y_c)^{-1} + (96y_c^3)^{-1} + O(y_c^{-5})$, of which the first two terms are reproduced by δ_a. Fig. 4 compares the exact phase (36) with its linear approximation (42) and with the semiclassical phase (43). All the phases depend on the parameter $y_c = q_c a = (4\pi\rho_2)^{1/2} a$. For $\rho_2 = 0.805 \times 10^{-5}$ Å^{-2} and $a = 333$ Å (the 5% to 95% of ρ_2 thickness is then about 2000 Å), $y_c \approx 3.35$.

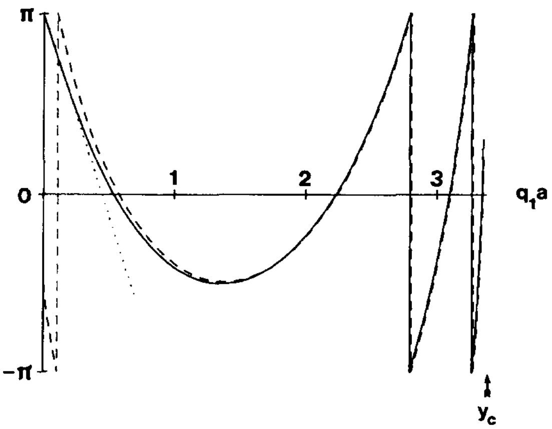

Fig. 4. Total reflection phase for the hyperbolic tangent profile: exact (solid curve), short-wave approximation (dashed curve) and linear part (dotted line). The ρ_2 value is 0.805×10^{-5} Å^{-2}, so that if $\lambda = 6.28$ Å, $\theta_c \approx 0.576°$.

4. The total phase difference between direct and reflected rays

In the preceding sections we explored the properties of the reflection phase δ, which relates to the motion in the z-direction, normal to the reflecting stratification. There is also a phase difference between the reflected and direct neutron waves due to motion in the x-direction. Fig. 5 shows the two paths.

The phase difference between the reflected and direct neutron rays can be broken up into the straight-path contributions (where the neutrons travel in vacuum), and the curved part contribution from within the reflecting stratification. The straight-path phase difference is

$$\Delta_s = \frac{2\pi}{\lambda}\{\sqrt{L_1^2 + H^2} + \sqrt{L_2^2 + h^2} - \sqrt{L^2 + (H-h)^2}\} = \frac{2\pi}{\lambda}\left\{-\Delta x + \frac{2Hh}{L} + \frac{(H^2 + h^2)\Delta x}{2L^2} + O(L^{-3})\right\}. \qquad (44)$$

The curved part contributes

$$\Delta_c = K\Delta x + \delta = \frac{2\pi}{\lambda}\Delta x \cos\theta + \delta. \qquad (45)$$

The tangential component K of the wave vector is a constant of the motion in a planar stratification. The value of Δx in the ray picture is (Ref. [4,

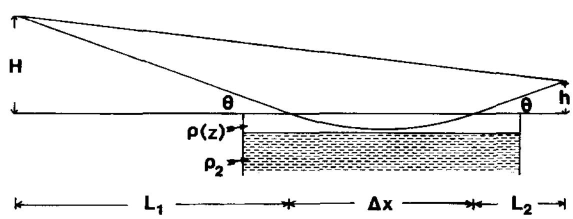

Fig. 5. Lloyd fringe formation in neutron total reflection. The direct ray has length $\sqrt{L^2 + (H-h)^2}$. The straight parts of the reflected ray have lengths $\sqrt{L_1^2 + H^2}$ and $\sqrt{L_2^2 + h^2}$. The horizontal distance from source to detector is $L = L_1 + L_2 + \Delta x$.

Eq. (10.50)])

$$\Delta x \approx 2\int_0^{z_0} \mathrm{d}z \cot\theta(z) = 2\int_0^{z_0} \mathrm{d}z\, K/q(z)$$
$$= \frac{K}{\sqrt{\pi}}\int_0^{z_0} \frac{\mathrm{d}z}{\sqrt{\rho(z_0)-\rho(z)}}. \qquad (46)$$

The last equality follows from Eqs. (3) and (5), which imply

$$q^2(z) = 4\pi[\rho(z_0) - \rho(z)]. \qquad (47)$$

The semiclassical value (46) may be obtained from the more general wave formula (Ref. [4, Eq. (10.51)])

$$\Delta x = -\frac{\mathrm{d}\delta}{\mathrm{d}K}, \qquad (48)$$

which applies when δ varies smoothly with K (thus the immediate neighbourhood of the critical angle or wavelength is excluded, because of the $(\theta - \theta_c)^{1/2}$ or $(\lambda_c - \lambda)^{1/2}$ singularities, which are universal for profiles of finite range, as shown in Section 10-2 of Ref. [4]). On using Eq. (1) in Eq. (48), with $q(z_0) = 0$ and

$$q^2(z) = \left(\frac{2\pi}{\lambda}\right)^2 - K^2 - 4\pi\rho(z), \qquad (49)$$

we regain Eq. (46). We have seen that Eq. (1) fails at grazing incidence, and is generally poor when there are discontinuities in the scattering density. Similar remarks apply to the corresponding formula (46) for Δx.

The quantity $2Hh/L$ is the leading term in the expansion of the geometric path difference in powers of L^{-1}. The leading terms in Δ which depend on the reflecting profile are

$$\Delta_{\text{profile}} = \delta + (K - 2\pi/\lambda)\Delta x. \qquad (50)$$

Since $K = (2\pi/\lambda)\cos\theta$, the small-angle expansion of this phase is

$$\Delta_{\text{profile}} = \pm\pi + c\theta - (\pi/\lambda)\theta^2\Delta x + \mathrm{O}(\theta^3). \qquad (51)$$

From Eq. (48) and $K = (2\pi/\lambda)(1 - \theta^2/2) + \mathrm{O}(\theta^4)$ we have, using Eq. (2),

$$\Delta x = -\frac{\mathrm{d}\delta}{\mathrm{d}K} = -\frac{\mathrm{d}\delta}{\mathrm{d}\theta}\frac{\mathrm{d}\theta}{\mathrm{d}K} = \frac{c\lambda}{2\pi\theta} + \mathrm{O}(\theta). \qquad (52)$$

Thus the effect of the transverse displacement on the phase is opposite to that of the reflection phase, in the term proportional to θ:

$$\Delta_{\text{profile}} = \pm\pi + \tfrac{1}{2}c\theta + \mathrm{O}(\theta^3). \qquad (53)$$

5. Summary and discussion

The semiclassical phase formula (1) fails at grazing incidence, both in value at $\theta = 0$ and in the θ-dependence for small θ.

For profiles of strictly finite range, the formula (15) gives the small-angle variation, and evaluates the constant c in $\delta = \pm\pi + c\theta + \mathrm{O}(\theta^3)$.

The semiclassical phase becomes accurate away from grazing incidence, provided the profile thickness is large compared to the neutron wavelength, and the profile is smooth.

The total phase difference has a term proportional to the lateral displacement of the neutrons during reflection, Δx. This term may be approximated by a semiclassical path integral, but only to the same accuracy as that of the semiclassical phase.

At grazing incidence the total profile phase has the same form as $\delta(\theta)$, with c reduced to $c/2$.

The Lloyd fringes in a given experiment are likely to be very closely spaced unless the detector is very far from the reflecting sample. For example, the contribution δ to the phase, in the case of homogeneous layer of 2000 Å thickness shown in Fig. 2, increases by five multiples of 2π between 0.3° and 0.5°. If a photographic film were to adjoin a layer impregnated with boron 10 or lithium 6, the neutron absorption reactions $^{10}\mathrm{B}(n, \alpha)$ or $^{6}\mathrm{Li}(n, \alpha)$ could be used to produce a latent image in the film, with a spatial resolution of the order of 10 μm or better. This may be a more convenient method of recording Lloyd mirror fringes than the use of conventional neutron detectors.

References

[1] See for example F.A. Jenkins and H.E. White, Fundamentals of Optics (McGraw-Hill, New York, 1950; 2nd ed.) Section 13.8.
[2] V.P. Gudkov, G.I. Opat and A.G. Klein, J. Phys.: Condens. Matter 5 (1993) 9013.

[3] B.E. Allman, A.G. Klein, K.A. Nugent and G.I. Opat. Eur. J. Phys. 14 (1993) 272; Appl. Opt. 33 (1994) 1806.
[4] J. Lekner, Theory of Reflection (Nijhoff/Kluwer, Dordrecht 1987).
[5] S.A. Werner and A.G. Klein, in: Methods of Experimental Physics, Vol. 23A (Academic Press, New York, 1986) ch. 4.
[6] J. Lekner, Physica B 173 (1991) 99, Eq. (37).
[7] M. Abramowitz and I. Stegun (eds.), Handbook of Mathematical Functions (US Government Printing Office, Washington, 1964) Section 10.4.
[8] L.D. Landau and E.M. Lifshitz, Quantum Mechanics (Pergamon, Oxford, 1965; 2nd ed.) Problem 3 of Section 25.